Virchows Arch. A Path. Anat. and Histol. 383, 167–179 (1979)

Virchows Archiv A

Ultrastructural Studies on the Evolution of Amyloidosis in the Cyclic Hematopoietic (CH) Dog*

Emilio A. Machado, J.B. Jones, and Robert D. Lange

University of Tennessee, Department of Medical Biology, Memorial Research Center, Center for Health Sciences, 1924 Alcoa Highway, Knoxville, Tennessee 37920, USA

Summary. Electron microscopy studies were made on tissues of cyclic hematopoietic (CH) dogs of various ages presenting a high incidence of spontaneous amyloidosis. The distribution and morphologic characteristics of amyloidosis in this animal model closely correspond to the secondary and familial forms of the disease in humans. Plasma cells and, particularly, macrophages presented marked changes during the evolution of amyloid deposition. Residual bodies in the macrophages contained abundant cell debris, a result of both endocytic and autophagocytic activities. Intracellular amyloid fibrils were not observed by conventional electron microscopy. A few reticular cells contained intracytoplasmic fibrils which were morphologically different from amyloid. There was no correlation between the amount of intracellular fibrils and the size of the extracellular amyloid deposits. On the contrary, a temporal association between the magnitude of the amyloid deposits and cytoplasmic changes in the macrophages at sequential stages of the evolution of the disease was evident. It is suggested that the hematopoietic defect in the CH dog could play an important role in the production of amyloidosis, making this animal an excellent experimental model for studies of that disease.

Key words: Amyloidosis – cyclic hematopoiesis – Animal model – Electron microscopy.

Introduction

Animal models are useful for performing sequential morphologic analyses on the deposition of amyloid. The grey collie, afflicted by hereditary cyclic hemato-

For offprints contact: Dr. Emilio A. Machado, University of Tennessee, Memorial Research Center, 1924 Alcoa Highway, Knoxville, TN 37920, USA

* Supported by Grants NIH RR00874, NIH HL 15647, and NIH FR5541 from the National Institutes of Health, DHEW

0340-1227/79/0383/0167/$02.60

poiesis (CH) (Lund et al., 1967; Ford et al., 1967; Dale et al., 1972), is suitable for this type of experimental study. This conclusion is supported by the following observations: 1) the CH dog shows a high incidence of spontaneous amyloidosis (Cheville et al., 1970; Gregory et al., 1977; Machado et al., 1978a) with a similar visceral distribution to that observed in secondary and familial types of the disease in humans; 2) amyloid deposits appear early in the life of the CH dog and gradually increase with age, independently of the severity of infections usually present. Furthermore, the lag period preceding the onset of the disease is remarkably short compared to other strains of dogs afflicted by amyloidosis associated with infections; 3) spontaneous resorption of amyloid, which is common in murine models (Williams, 1967; Polliack et al., 1970) and rarely found in humans (Lowenstein and Gallo, 1970; Dikman et al., 1977), does not occur in CH dogs; 4) among mammal animal models, the dog presents remarkable physiopathological similarities with humans. In addition, the large size of the CH dog and its long life span under proper conditions make it possible to perform sequential studies over an extended period of time in the same animal.

A systematic characterization of the ultrastructural changes occurring over the evolution of amyloidosis in the CH dog is necessary for further experimental use of this unique animal model. Most of the studies published to date, however, deal with post-mortem findings in a limited number of dogs.

The purpose of this paper is to describe the ultrastructural features of amyloid deposition in the CH dog at sequential stages and to discuss some aspects of the temporal association between cellular changes and evolution of the amyloid deposits.

Material and Methods

Samples for light and electron microscopy studies were taken from spleen, kidney, and liver at autopsies of CH dogs of various ages from the colony maintained at the University of Tennessee Memorial Research Center (UTMRC) (Machado et al., 1978a; Jones et al., 1975). Tissues from breeders and normal littermates were used as controls.

The presence of amyloid in tissues was routinely detected by the green birefringency under polarized light alfter alkaline Congo red staining (Missmahl and Hartwig, 1953).

Small blocks of tissue were fixed in 3% glutaraldehyde in 0.05 M cacodylate buffer, post-fixed in osmium tetroxide, and processed by conventional procedures for electron microscopy. Tissues were also fixed in glutaraldehyde with 1% lanthanum nitrate added (Shaklai and Tavasoli, 1977). Thick sections (1 μ) were used for selecting the appropriate blocks by light microscopy. Thin sections were cut on a Porter-Blum MT2-B ultramicrotome, stained with lead citrate and uranyl acetate, and examined under a Zeiss EM9-S electron microscopy. Sections of tissues fixed with lanthanum were examined unstained.

Isolation of Amyloid Fibrils. For further characterization, amyloid fibrils were extracted from the spleen of a CH dog following the method of Glenner et al. (Glenner et al., 1972). Drops of an aqueous solution of purified fibrils, spread on Formvar-copper grids, were "negatively" stained with 2% PTA solution or metal coated for electron microscopy examinations.

The molecular weight of this amyloid was determined in an extract of purified fibrils.

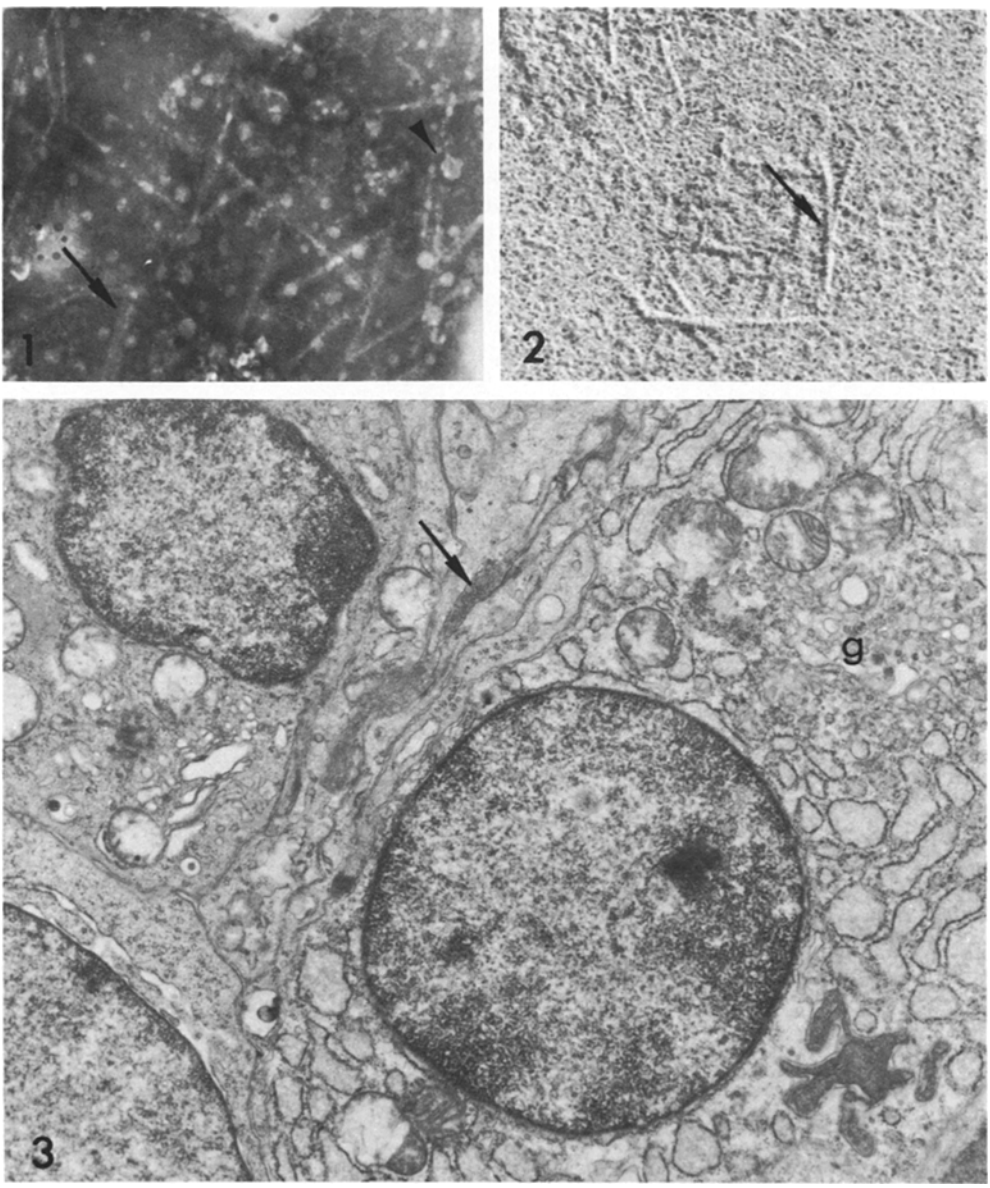

Fig. 1. Negatively stained fibrils isolated from the amyloid-laden spleen of a CH dog. Double filaments are noted in some fibrils *(arrow)*. Arrowhead indicates ring-shaped (P component) structure (2% PTA, ×136,400)

Fig. 2. Metal coated appearance of the same fibrils shown in Figure 1. A separation of individual filaments *(arrow)* is apparent in one fibril (×29,500)

Fig. 3. Plasma cell in the spleen with hyperplastic Golgi apparatus (*g*) and dilated RER in the vicinity of an early extracellular amyloid deposit *(arrow)*. It can be noted that the amyloid substance is separated from the plasma cell by cytoplasmic extension from other cells (×13,160)

Results

General Pathologic Findings. We have previously described the general pathologic characteristics of amyloidosis in the CH dog. Briefly, the incidence and extent of amyloidosis in the tissues of the CH dog were consitently associated with age. Early amyloid deposits were found in CH dogs as young as 15 weeks of age and gradually increased thereafter. More than 80% of the dogs over 24 weeks of age displayed widespread amyloidosis. Splenic follicles, hepatic portal and sinusoidal spaces, and renal glomeruli were the areas more commonly involved by amyloid deposits. Adrenals, gastrointestinal tract, and pancreas were occasionally affected. Heterozygous breeders and normal littermates, which do not show hematopoietic cycling, did not have any signs of amyloidosis.

Amyloid Fibrils. Isolated fibrils appeared as rigid rods, approximately 75 Å in diameter, and were formed by the coupling of thinner units (Figs. 1 and 2). Round structures were randomly distributed; some were composed of several small globular units surrounding an empty area, corresponding morphologically to the "P" component.

The amino acid sequence of this amyloid has not yet been determined but it has a low molecular weight (8,500).

Ultrastructural Cellular Changes. Plasma cells, appearing in the vicinity of amyloid deposition, had highly developed rough endoplasmic reticulum (RER) (Fig. 3). The dilated cisternae contained a flocculent material of low electron density. In some of the cisternae, the content was homogenous and dark. Ribosomes were mainly attached to the membranes of the RER; free particles or clusters in the cytoplasmic ground substance were scarce. The Golgi apparatus was prominent, composed of numerous large and small vesicles and flattened sacs, and occupied an extensive area of the cytoplasm. These characteristics of the plasma cells were similar at both early and advanced stages of amyloid deposition.

The macrophages presented marked cytoplasmic changes which were particularly evident in the marginal areas of the splenic follicles. At early stages of amyloid deposition, these cells displayed numerous lysosomes of varied size and double-membrane-limited residual bodies (Fig. 4). The residual bodies, seen at various stages of evolution, contained fragmented organelles and filamentous aggregates. Multiple small vesicles, derived from the smooth endoplasmic reticu-

Fig. 4. Splenic macrophages in the vicinity of an early extracellular amyloid deposit *(arrowhead)*. Arrows indicate lysosomes of varied sizes. A medium sized residual body (*rb*) and glycogen accumulation (*gl*) are also noted. RER strands surround a mitochondrium (*m*) in the initial stages of the formation of an autophagosome (× 28,500)

Fig. 5. Splenic macrophages at a more advanced stage of amyloid deposition. Numerous large and dense lysosomes occupy the cytoplasm. A residual body contains "fingerprint degeneration" (*fd*) material and myelin figures. Fusion of the residual body with a lysosome and continuity with smooth vesicles are indicated by an arrow (× 28,500)

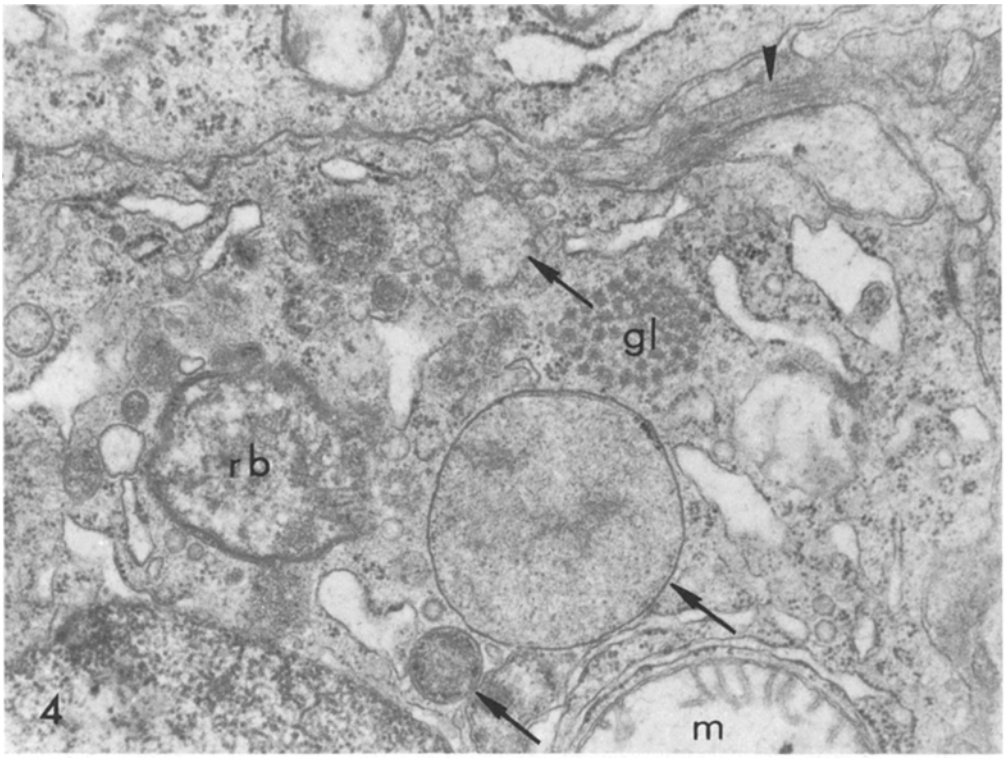
gl
rb
m
4

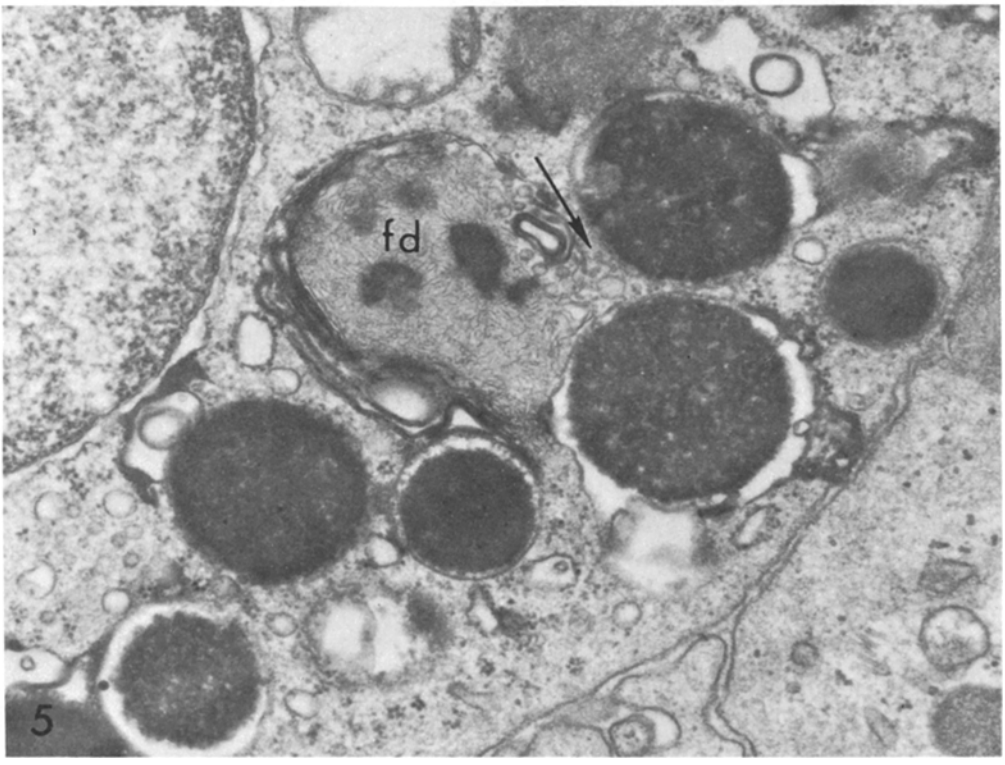
fd
5

lum (SER) or Golgi apparatus, appeared around the lysosomes and close to the plasma membrane. The RER displayed partially degranulated, dilated cisternae; small clusters of detached ribosomes were randomly distributed in the cytoplasm. Glycogen accumulations were present in some macrophages.

These changes became more accentuated during the evolution of amyloid deposition. Thus, large residual bodies enclosing myelin figures, filamentous debris, and lipid droplets were the dominant characteristic in the cytoplasm of macrophages at advanced stages of the disease (Figs. 5–7). A few residual bodies contaned electron dense material with a whorled pattern similar to the "fingerprint degeneration" of the ER (Fig. 5). These whorl arrangement appeared connected with smooth vesicles in areas where the membranes of residual bodies were incomplete. Fusion between primary lysosomes and residual bodies was often noted.

Elongated bodies bound by a double membrane and containing tightly packed, electron dense material were occasionally found in macrophages (Fig. 8). These inclusions apparently corresponded to tangential sections of cytoplasmic invaginations of amyloid fibrils.

The reticular cells did not show marked abnormalities during the evolution of amyloidosis. The number of cytoplasmic organelles in these cells was scarce, presenting a moderate dilation of strands of RER and a few SER vesicles (Fig. 9).

Bundles of low electron density fibrils, displaying a parallel, waving pattern, were observed within some reticular cells (Fig. 10). These fibrils displaced the organelles without defined structural connections with them. Morphologically, they were different from the electron dense amyloid fibrils which have a typical non-branching crossed pattern. Their general appearance resembled the collection of intracellular microtubules or fibrils seen in some tumors without associated amyloidosis (Fig. 11).

Although the reticular and endothelial cells did not show the marked cytoplasmic changes seen in macrophages, they had an extensive spatial relationship with the extracellular amyloid deposits.

Evolution of the Amyloid Deposits. Early amyloid deposits appeared as extracellular accumulations of an electron-dense material with fibrillar areas between the outer membranes of reticular and endothelial cells and within the spaces

Fig. 6. Abundant residual bodies in a macrophage (*M*) close to extensive amyloid deposition in the marginal area of the spleen. The amyloid (*am*) deposits show a micronodular appearance and encroach into the neighboring cells (×6,555)

Fig. 7. Detail of residual bodies shown in Figure 6. They are bounded by double membranes and contain filamentous debris and black lipid droplets. Identifiable amyloid fibrils are not observed within the residual bodies or the cytoplasm of the macrophage (×16,450)

Fig. 8. Amyloid (*am*) micronodular deposition advancing into the red pulp of the spleen. A group of erythroblasts is noted in the area. Dense intracellular inclusion *(arrow)* in a cytoplasmic extension (24,560)

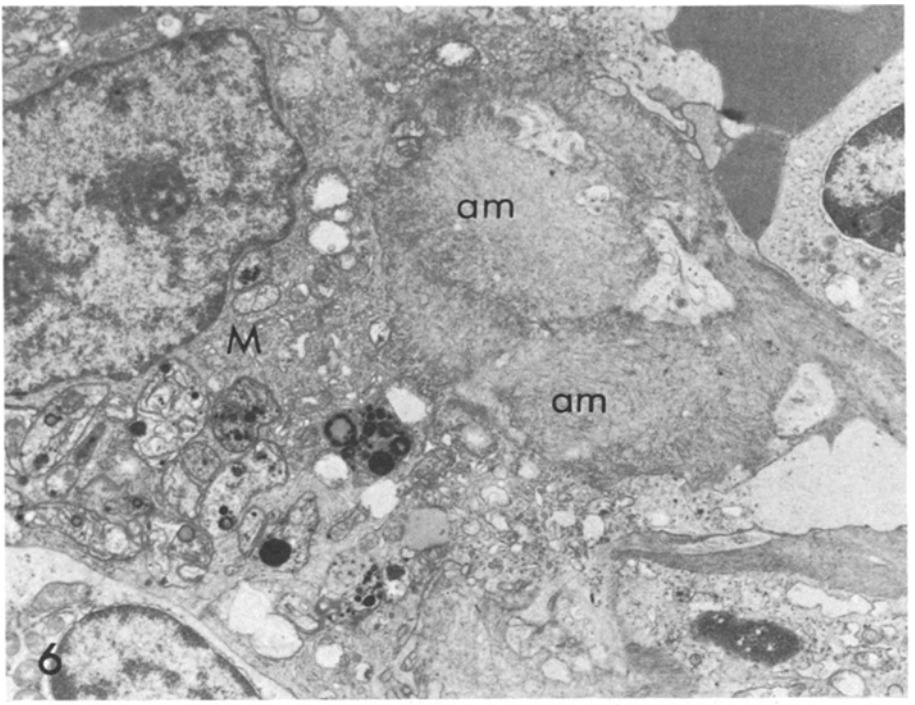
am
M
am
6

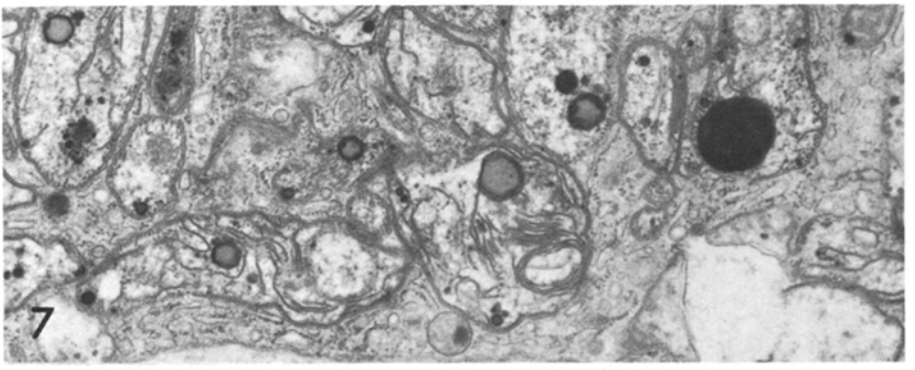
7

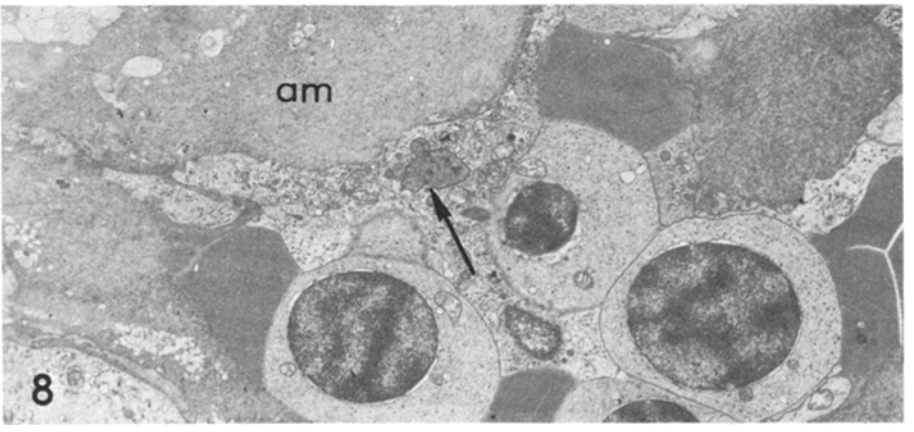
am
8

formed by interdigitation of the processes of these cells (Fig. 9). Amyloid deposits appeared to have an eccentric increase in size by apposition of new fibrils. Macrophages and plasma cells appeared in the vicinity of early amyloid deposits but were often separated from the fibrils by thin cytoplasmic prolongations of the reticular and endothelial cells.

In the kidney, the early small deposits under the endothelium and among the mesangial cells evolved to form large accumulations which compressed the mesangial cells of the glomerulus and surrounded isolated areas of cytoplasm and foot processes (Fig. 12). Amyloid was also noted in the interstitial tissue surrounding the renal tubules. Fibrils were not found in the subepithelial area of the tubules. In the liver, early amyloid deposits were observed in the interstitial tissue of the portal area. At more advanced stages, amyloid deposits in the space of Disse had a nodular configuration and displaced the endothelial and Kupffer's cells lining the sinusoids. The deposits compressed the hepatocytes, producing multiple indentations in their sinusoidal aspect (Fig. 13).

Amyloid deposits in the marginal areas of the splenic follicles were formed by the coalescence of several fibrillar micronodules (Figs. 6 and 8). Identical morphology was noted in those deposits which extended outwardly to the red pulp. The central portion of the deposits was usually lighter than the peripheral area which appeared formed by radiating fibrils encroaching into the surrounding cells. Variations in electron density and the pattern of fibrillar arrangements suggested that the nodules of amyloid fibrils were formed by successive concentric layer deposits.

Section stained with lanthanum showed areas of discontinuity of the plasma membranes of the reticular cells surrounding amyloid deposits (Fig. 14). In these areas, there was no clear separation between the metallic precipitates of the outer border of the cell membrane and those intermingled with the amyloid fibrils. Except for the focal alterations of the peripheral membrane associated with the amyloid deposits, the reticular cells did not show cytoplasmic changes or inclusions.

Fig. 9. Reticular cell (*R*) and a macrophage (*M*) surrounding initial deposits of amyloid *(arrow)*. The cytoplasms of the reticular cells do not show remarkable changes (× 21,850)

Fig. 10. Fine, waving intracellular fibrils *(arrow)* in a reticular cell. Organelles appear dispersed by the bundles of fibrils that occupy the cytoplasmic matrix (18,800)

Fig. 11. Intracellular fibrils *(arrows)*, similar to those shown in Figure 10, in a tumor cell *(myelosarcoma)* without amyloid deposition (× 19,000)

Fig. 12. Extensive accumulation of amyloid compressing an epithelial cell (*Ep*) and foot processes *(arrows)* in a glomerulus at advanced stage of amyloidosis (× 20,900)

Fig. 13. Micronodular amyloid deposits in the space of Disse. Cytoplasmic alteration of the hepatocytes are indicated by arrows. (*L*) lumen of sinusoid, (*K*) Kupffer cell (× 4,000)

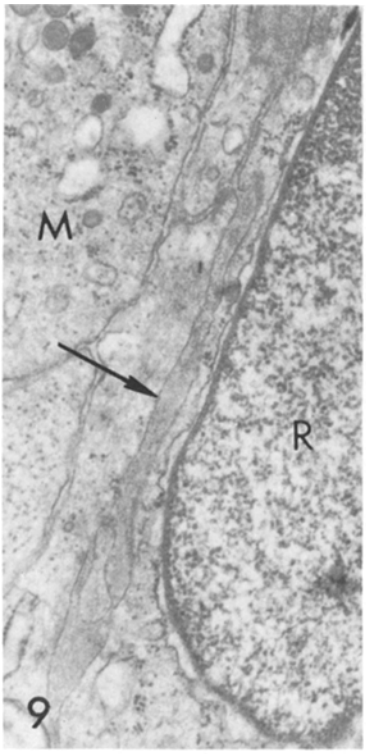
M
R
9

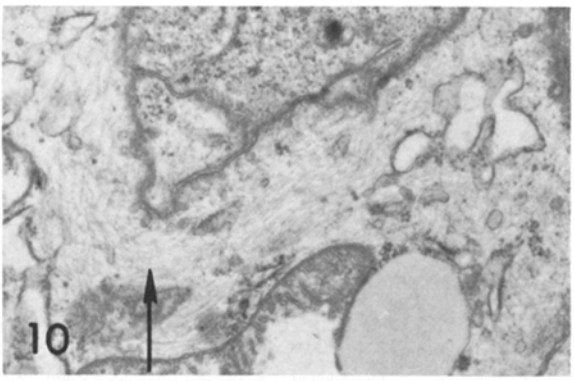
10

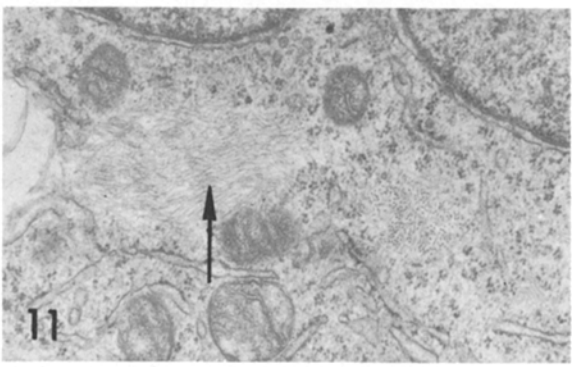
11

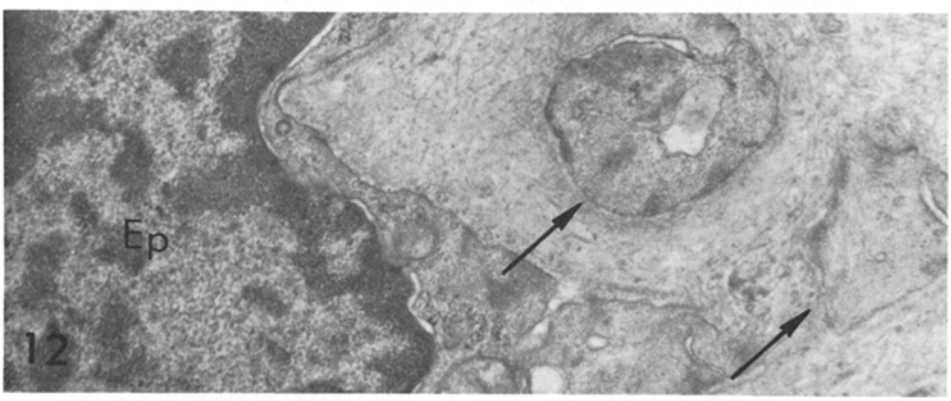
Ep
12

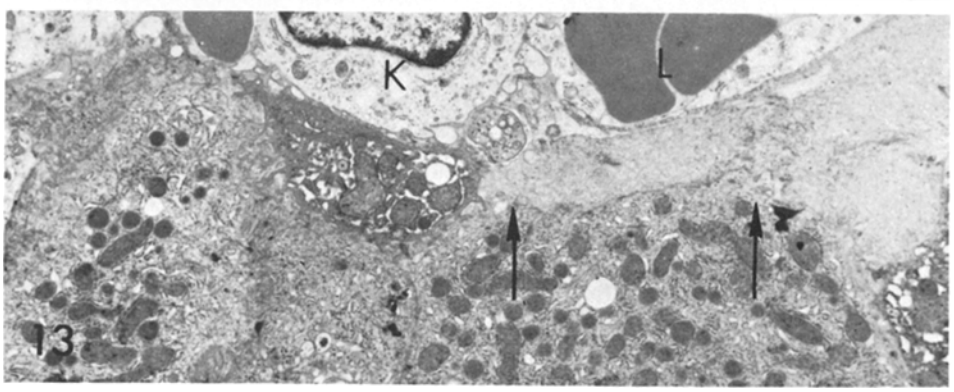
K
L
13

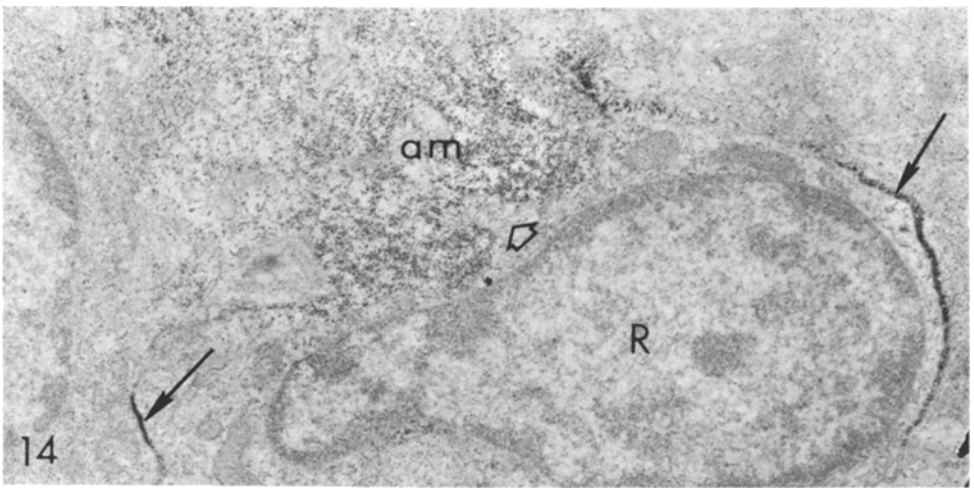

Fig. 14. Unstained section of spleen fixed with lanthanum added. The solid arrows indicate the normal pattern of lanthanum deposition in the cell membrane of a reticular cell (*R*). These is an area of discontinuity of the membrane *(open arrow)* adjoining an extracellular amyloid deposit (*am*). Metallic precipitates are present amidst amyloid fibrils groups. The characteristics of the reticular cell are not markedly modified (× 16,450)

Discussion

As was previously reported (Gregory et al., 1977; Machado et al., 1978), the visceral distribution and morphologic characteristics of amyloidosis in CH dogs are remarkably similar to the secondary and familial forms of the disease in humans. The amino acid sequence of this amyloid has not yet been determined; however it has been found to have a low molecular weight.

The ultrastructural studies confirmed the similarities between amyloid deposition in the spleen, liver, and kidneys of the CH dog and the systemic forms of the condition in humans. In the kidneys, besides the typical glomerular involvement, amyloid fibrils were also found in the peritubular areas. These deposits did not have the subepithelial distribution noted in other animal models (Cohen and Shirahama, 1971), but were observed in the interstitial tissue as in human renal amyloidosis (Jao and Pirani, 1972).

Our findings indicate that cytoplasmic changes in the macrophages and, to a lesser extent, in the plasmocytes are observed even at the earlier stages of extracellular amyloid deposition. Signs of endocytic and autophagic activities in the macrophages became more marked during the evolution of the disease. Although these could be considered merely coincidental phenomena, the consistent association of the magnitude of changes in the macrophages with the increase of amyloid deposits is worthwhile being taken into account.

At well-advanced stages of the disease, the expansive growth of the amyloid deposits produced necrotic changes in the parenchymal tissues of kidneys and liver. The necrotic changes induced an active removal of cell debris by the

macrophages, readily detected by electron microscopy. However, phagocytosis of amyloid fibrils (Zucker-Franklin, 1970) or the presence of amyloid fibrils within the lysosomes observed under experimental conditions (Shirahama and Cohen, 1971), were not found in the CH dog. Obviously, phagocytosis of breakdown products of amyloid fibrils cannot be ruled out just on the basis of morphologic observations; however, it could be speculated that the rate of phagocytosis of denatured amyloid, not detectable by conventional electron microscopy, would not be significant because amyloid deposition in the CH dog is a continuous process leading to severe parenchymal damage regardless of the presence of numerous active macrophages.

Intracellular fibrils have been observed during the course of amyloidogenesis in animal models (Ranløv and Wanstrup, 1967) and in humans (Kjeldsberg et al., 1977; Zucker-Franklin and Franklin, 1970). The fibrils found in reticular cells of the CH dog did not show the ultrastructural characteristics of amyloid. It must also be noted that the number of reticular cells containing a discrete amount of fibrils was small and did not present signs of cell injury which could be associated with a holocrine mechanism of amyloid deposition. The interpretation of the nature of the intracellular fibrils by morphologic means is difficult, but the observations suggest that they are more likely related to microtubular proliferation than to amyloid formation. We have found similar fibrils in human malignant myelogenous cells transplanted into mice (Machado et al., 1978b). Amyloidosis was not observed in these experimental animals.

Another point which deserves comment concerns the structural aspect of the extracellular amyloid deposits which appeared to be formed by the coalescence of several micronodules. The differences between the electron density and fibrillar arrangement of the central and peripheral areas of the nodules suggested that they increase in size by apposition of successive layers of amyloid substance on a primitive core. The magnitude of these extracellular deposits of amyloid substance does not agree with the sparse intracellular fibrils observed in some reticular cells.

The lanthanum precipitates revealed discontinuities in the membranes of the reticular cells surrounding amyloid deposits. Cytoplasmic changes in these cells were, however, slight and accumulations of intracellular fibrils were not observed. The appearance of metallic precipitates among bundles of amyloid fibrils may be due to the displacement and aggregation of mucopolysaccharides of the extracellular ground substance. It is known that mucopolysaccharides do not participate in the chemical composition of amyloid.

Lymphocytes, plasma cells, and macrophages (Cohen et al., 1975), as well as granulocytes (Rosenthal and Sullivan, 1979), are thought to be involved in the pathogenesis of the various forms of amyloidosis in humans and experimental animals. The abnormalities of the blood cell series inherent to the CH syndrome have not yet been well defined and are under study in this and other laboratories. However, the premature development of amyloidosis in the CH dog would indicate that the role of antigenic stimulation of infections may be facilitated by functional defects of the bone marrow and lymphoid cells. This indicates that the CH dog may represent an excellent model for the study of amyloid disease in humans. The origin of this amyloid remains

to be determined by future studies. Glenner and Page (Glenner and Page, 1976) singled out this animal model as one of "particular promise" for the study of amyloidosis. Yet, to date, the value of the CH dog for experimental studies on that disease has barely been explored.

Acknowledgements. We are grealy indebted to Dr. Alan Solomon (University of Tennessee Memorial Research Center) for the isolation of amyloid fibrils, and to Dr. Peter D. Gorevic (State University of New York at Stony Brook) for the determination of the molecular weight. We also want to acknowledge the excellent technical and secretarial assistance of Ms. Patricia Maxwell and Ms. Lucille Simpson, respectively.

References

Cheville, N.F., Cutlip, R.C. Moon, H.W.: Microscopic pathology of the gray collie syndrome. Cyclic neutropenia, amyloidosis, enteritis, and bone necrosis. Pathol. Vet. **7**, 225–245 (1970)

Cohen, A.S., Shirahama, T.: Ultrastructural studies of renal peritubular amyloid experimentally induced in guinea pigs. II. Tubular epithelial cells. Arthritis Rheum. **14**, 429–439 (1971)

Cohen, H.J., Lessin, L.S., Hallal, J., Burkholder, P.: Resolution of primary amyloidosis during chemotherapy studies in a patient with nephrotic syndrome. Ann. Intern. Med. **82**, 466–473 (1975)

Dale, D.C., Alling, D.W., Wolff, S.M.: Cyclic hematopoiesis: The mechanism of cyclic neutropenia in grey collie dogs. J. Clin. Invest. **51**, 2197–2204 (1972)

Dikman, S.H., Kahn, T., Gribetz, D., Churg, J.: Resolution of renal amyloidosis. Am. J. Med. **63**, 430–433 (1977)

Ford, L.: Hereditary aspects of human and canine cyclic neutropenia. J. Hered. **60**, 293–299 (1967)

Glenner, G.G., Harada, M., Isersky, C.: The purification of amyloid fibril proteins. Prep. Biochem. **2**, 39–51 (1972)

Glenner, G.G., Page, D.L.: Amyloid, amyloidosis and amyloidogenesis. Int. Rev. Exp. Pathol. **15**, 1–92 (1976)

Gregory, R.S., Machado, E.A., Jones, J.B.: Animal model of human disease: Amyloidosis associated with canine cyclic hematopoiesis in the gray collie dog. Am. J. Pathol. **87**, 721–724 (1977)

Jao, W., Pirani, C.L.: Renal amyloidosis: Electron microscopic observations. Acta Pathol. Microbiol. Scand. [A] **233**, 217–227 (1972)

Jones, J.B., Lange, R.D., Jones, E.S.: Cyclic hematopoiesis in a colony of dogs. J. Am. Vet. Med. Assoc. **166**, 365–367 (1975)

Kjeldsberg, C.R., Eyre, H.J., Totzke, H.: Evidence of intracellular amyloid formation in myeloma. Blood **50**, 483–504 (1977)

Lowenstein, J., Gallo, G.: Remission of the nephrotic syndrome in renal amyloidosis. N. Engl. J. Med. **282**, 128–132 (1970)

Lund, J.E., Padgett, G.A., Ott, R.L.: Cyclic neutropenia in grey collie dogs. Blood **29**, 452–461 (1967)

Machado, E.A., Gregory, R.S., Jones, J.B., Lange, R.D.: The cyclic hematopoietic dog: A model for spontaneous secondary amyloidosis. A morphologic study. Am. J. Pathol. **92**, 23–34 (1978)

Machado, E.A., Lozzio, B.B., Lozzio, C.B., Aggio, M.C.: Heterotransplantation of the K562 cell line derived from a patient with chronic myeloid leukemia. In: Advances in comparative leukemia research 1977, Bentvelzen, P. et al. (eds.), pp. 418–421. Amsterdam: Elsevier/North-Holland 1978

Missmahl, H.P., Hartwig, M.: Polarisationsoptische Untersuchungen an der Amyloidsubstanz. Arch. Pathol. Anat. **324**, 489–508 (1953)

Polliack, A., Laufer, A., Tal, C.: Studies on the resorption of experimental amyloidosis. Br. J. Exp. Pathol. **51**, 236–241 (1970)

Ranløv, P., Wanstrup, J.: Ultrastructural investigations on the cellular morphogenesis of experimental mouse amyloidosis. Acta Pathol. Microbiol. Scand. [A] **71**, 575–591 (1967)

Rosenthal, C.J., Sullivan, L.: Serum amyloid A: Evidence for its origin in polymorphonucleated leukocytes. J. Clin. Invest. (in press)
Shaklai, M., Tavassoli, M.: A modified technique to obtain uniform precipitation of lanthanum tracer in the extracellular space. J. Histochem. Cytochem. **25**, 1013–1015 (1977)
Shirahama, T., Cohen, A.S.: Lysosomal breakdown of amyloid fibrils by macrophages. Am. J. Pathol. **63**, 463–486 (1971)
Williams, G.: Histological studies in resorption of experimental amyloid. J. Pathol. Bacteriol. **94**, 331–336 (1967)
Zucker-Franklin, D.: Immunophagocytosis of human amyloid fibrils by leukocytes. J. Ultrastruct. Res. **32**, 247–257 (1970)
Zucker-Franklin, D., Franklin, E.C.: Intracellular localization of human amyloid by fluorescence and electron microscopy. Am. J. Pathol. **59**, 23–41 (1970)

Received April 18, 1979